Microchimica Acta (2023) 190:399
https://doi.org/10.1007/s00604-023-05952-3

ORIGINAL PAPER

Ti^{4+} functionalized β-cyclodextrin covalent organic framework as a new immobilized metal ion affinity chromatography platform for selective capture of phosphorylated peptides and exosomes

Bing Wang[1] · Xiaoya Zhang[1] · Baichun Wang[1] · Quanshou Feng[1] · Yiting Luo[1] · Weimin Wang[1] · Chuan-Fan Ding[1] · Yinghua Yan[1]

Received: 1 May 2023 / Accepted: 9 August 2023 / Published online: 18 September 2023

Abstract

A Ti^{4+} functionalized β-cyclodextrin covalent organic framework nanoparticle (named as β-CD-COF@Ti^{4+}) was synthesized using a one-pot method successfully realizing the enrichment of phosphorylated peptides and exosomes based on the immobilized metal ion affinity chromatography strategy. The functionalized β-CD-COF@Ti^{4+} exhibited superior performance on the enrichment of phosphopeptides, including high selectivity (1:1000), low detection limit (0.5 fmol), and loading capacity for phosphopeptides (100 $mg{\cdot}g^{-1}$). After treatment with β-CD-COF@Ti^{4+}, 9 phosphopeptides from defatted milk, 29 phosphopeptides related to 23 phosphoproteins from normal group serum, and 24 phosphopeptides related to 22 phosphoproteins from the serum of uremia patients were captured. Through the analysis of Gene Ontology, the captured phosphoprotein is closely related to kidney disease, including lipoprotein metabolism, very-low-density lipoprotein particle, high-density lipoprotein particle, and lipid binding activity process. Furthermore, western blot verification showed that this nanoparticle could successfully capture exosomes from human serum. This study demonstrates great prospects for the enrichment of phosphopeptides and exosomes from actual bio-samples.

Keywords β-Cyclodextrin covalent organic frameworks · Exosomes · Phosphopeptides · Phosphoproteins · Enrichment

Introduction

Exosomes, widely distributed in body fluids such as blood and urine, are secreted by various living cells and play an irreplaceable role in intercellular molecular transport and signal transduction [1–5]. Studies have shown that exosomes are associated with pathological changes in some diseases and may become related biomarkers [6–8]. Phosphorylation is a fundamental and significant protein post-translational modification [9], involved in various processes such as cell metabolism, cell apoptosis, energy conversion, and signal transduction [10, 11]. Some studies have demonstrated that phosphorylation mediates the occurrence and development of some diseases by participating in exosome biogenesis [12]. Exosomal phosphorylated proteins may be potential biomarkers to achieve early diagnosis of diseases [13]. Therefore, the analysis of exosomal phosphopeptides is beneficial to elucidate the pathogenesis of related diseases.

Currently, the immobilized metal ion affinity chromatography (IMAC) strategy is one of the most popular strategies for phosphopeptide enrichment [14, 15]. Numerous substrates have been developed to fix metal ions, such as graphene, mesoporous silica, and metal/covalent organic frameworks [16–18]. However, the most prepared IMAC materials not only need complex steps but also have finite binding sites for metal ions due to the limitations of the substance themselves. In addition, for most substrates used to prepare IMAC materials, due to the limited hydrophilicity and small specific surface area, it is necessary to select suitable organic ligands to construct IMAC materials with

✉ Weimin Wang
wwm1026632948@hotmail.com

✉ Chuan-Fan Ding
dingchuanfan@nbu.edu.cn

✉ Yinghua Yan
yanyinghua@nbu.edu.cn

[1] Key Laboratory of Advanced Mass Spectrometry and Molecular Analysis of Zhejiang Province, School of Materials Science and Chemical Engineering, Institute of Mass Spectrometry, Ningbo University, Ningbo 315211, China

high hydrophilicity and large specific surface area. Covalent organic frameworks (COFs) have attracted extensive interest due to the simple synthesis procedure, good chemical stability, and abundant functional groups [19, 20]. Among the many types of organic structural units, β-CD is a very promising ligand for constructing COF due to its rich groups. By braiding β-CD into a framework through reticulation chemistry, the resulting β-CD-COF has high chemical stability [21], which has greatly broadened its applications in proteomics. Therefore, β-CD-COF carries abundant chelation sites favorable for the chelation of more metal ions and has the potential to be an effective IMAC-based nanomaterial to achieve the enrichment of phosphorylated peptides and exosomes.

Herein, a Ti^{4+} functionalized β-cyclodextrin covalent organic framework was developed via a new one-pot method and used as an IMAC platform for the enrichment and separation of phosphorylated peptides and exosomes. We prepared β-CD-COF by using 2,3,4-trihydroxybenzaldehyde (THBA), p-phthalaldehyde (TPA), and Heptakis-(6-amino-6-deoxy)-cyclodextrin (Am7CD) via Schiff base reaction under mild reaction conditions. Subsequently, by means of the abundant cis dihydroxyl groups carried by the organic ligand THBA introduced in the prefabricated framework, a large number of Ti^{4+} was firmly fixed onto the β-CD-COF substrate, thus endowing the proposed material with adsorption capacity for phosphopeptides. Furthermore, benefiting from the novel organic ligand structure and the introduction of metal ions, the functionalized β-CD-COF@Ti^{4+} provides a new pathway to detect and separate phosphorylated peptides and exosomes.

Experimental section

Chemicals

p-Phthalaldehyde (TPA), 2,3,4-trihydroxybenzaldehyde (THBA), 2,5-dihydroxybenzoic acid (DHB), acetic acid (HAc), and phosphate buffer solution (PBS) were purchased from Macklin. Trypsin, albumin from bovine serum (BSA), ethanol (EtOH), acetonitrile (ACN), and β-casein (98%) were bought from Sigma-Aldrich. Heptakis-(6-amino-6-deoxy)-β-cyclodextrin (Am7CD), trifluoroacetic acid (TFA), titanic sulfate, iodoacetamide (IAA), and dithiothreitol (DTT) were bought from Aladdin. The serums of patients with uremia were obtained from the Affiliated Hospital of Medical School, Ningbo University, with the approval from its Ethics Committee (KS20227002).

Synthesis of β-CD-COF

A total of 114.4 mg of Am7CD, 87 mg of TPA, and 78.2 mg of THBA were dispersed ultrasonically in a centrifuge tube (10 mL) containing ethanol (2.5 mL) and water (2.5 mL), followed by the addition of 0.05 mL of HAc (176 mM). After stewing at room temperature for 50 h, the resulted β-CD-COF was collected and thoroughly washed with water and EtOH 3 times, respectively. The β-CD-COF was dried under vacuum for 24 h at 50 °C.

Synthesis of β-CD-COF@Ti^{4+}

Firstly, 40 mg of β-CD-COF was added into 12 mL of titanium sulfate solution (100 mM) and oscillated for 4 h at room temperature. Then, the synthesized β-CD-COF@Ti^{4+} was dried under vacuum.

β-CD-COF@Ti^{4+} was synthesized by a simple two-step procedure (Fig. 1). First of all, Am7CD, THBA, and TPA were added into the mixed solution of water and ethanol, and the imide condensation reaction was carried out under the catalysis of acid to obtain β-COF. Then, the solid material was immersed in a certain concentration of the solution of titanic sulfate, and the Ti^{4+} was chelated with the hydroxyl group in THBA to acquire the Ti^{4+} functionalized β-cyclodextrin covalent organic framework (β-CD-COF@Ti^{4+}).

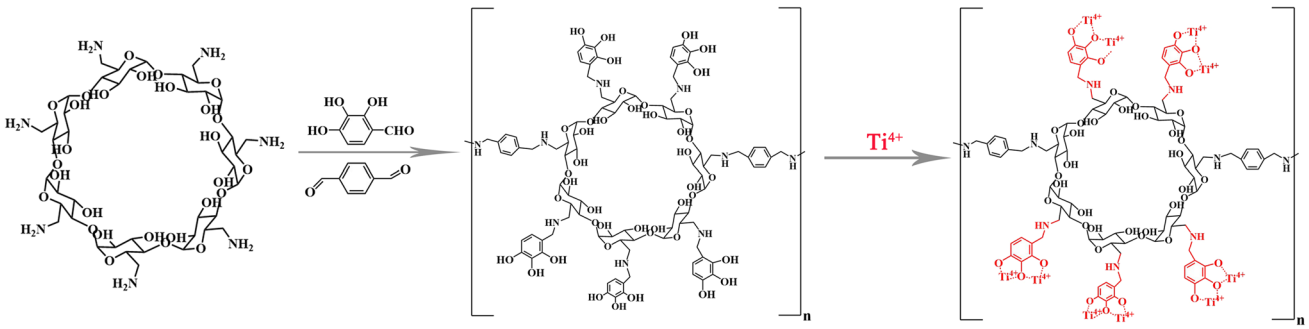

Fig. 1 The schematic representation of the preparation process of β-CD-COF@Ti^{4+} composites

Enrichment of phosphopeptides from standard protein digests

β-CD-COF@Ti^{4+} (100 μg) was added into the loading buffer (50% ACN, 0.5% TFA) containing β-casein digest (2 μL). The material loaded with the phosphopeptides was washed with loading buffer several times after vibrating at 37 °C for 45 min. Then, 10 μL of eluent (0.4 mol/L NH_3•H_2O) was poured, and the solution was shaken for 30 min at 37 °C. The eluent was obtained and analyzed by matrix-assisted laser desorption/ionization time-of-flight mass spectrometry (MALDI-TOF MS).

Enrichment of phosphopeptides from biological samples

β-CD-COF@Ti^{4+} (1 mg) was put into the loading buffer (100 μL) including 2 μL of human serum. The mixture was washed five rounds with loading buffer after vibrating at 37 °C for 45 min. Next, 2 × 10 μL of eluent was incubated at 37 °C for 0.5 h. Then, the eluent was lyophilized and desalted for further experiments. The pretreatment process of serum could be seen in supporting information.

Except for the practical biological samples (20 μL), the steps for enriching phosphopeptides from defatted milk were the same as the above experiments for enriching phosphopeptides from human serum. The pretreatment of defatted milk could be seen in supporting information.

Enrichment of the exosomes from human serum

β-CD-COF@Ti^{4+} (3 mg) was added into the centrifuge tube containing 100 μL of human serum and vibrated for 45 min at 4 °C. The pretreatment of serum could be seen in supporting information. Then, the material was washed with low-temperature PBS for 3 times. Subsequently, the eluent (10 μL) was put in a centrifuge tube and vibrated at 4 °C for 0.5 h. Lastly, the mixture was obtained and used for follow-up experiments.

Results and discussion

The optimization of synthesis conditions and characterization of β-CD-COF@Ti^{4+}

A range of characterization experiments were performed to verify the synthesis of the β-CD-COF@Ti^{4+}. Scanning electron microscopy (SEM) and transmission electron microscopy (TEM) images of β-CD-COF and β-CD-COF@Ti^{4+} showed that the materials were nanospheres with a diameter of about 500 nm (Fig. S1 and Fig. 2). The energy dispersive X-ray spectra (EDX) demonstrated the presence of Ti^{4+} (Fig. S2). Besides, Fourier-transform infrared spectroscopy (FT-IR) was carried out (Fig. S3). The peaks at 1693 cm^{-1}, 1769 cm^{-1}, and 1785 cm^{-1} assigned to the vibration of C=O disappeared, and the peaks at 1597 cm^{-1} and 3322 cm^{-1} attributed to the vibration of C=N appeared [22–24], indicating the success of the Schiff base reaction.

To optimize the synthesis of β-CD-COF, the materials were prepared with different molar ratios (β-CD: THBA = 1:2, 1:5, 1:10). According to the best experimental results in Fig. S4, the ligand ratio was determined to be 1:5 in subsequent experiments. The analytical process for the optimization of the ratio of β-CD-COF materials can be obtained from supporting information.

Application of β-CD-COF@Ti^{4+} for the enrichment of phosphopeptides from standard protein digests

Trypsin digested β-casein was employed as an enrichment sample to verify the enrichment performance of β-CD-COF@Ti^{4+}. In order to obtain the best enrichment ability for phosphopeptides, the optimal incubation time (15 min, 30 min, 45 min, and 60 min) was studied. MALDI-TOF MS analysis results indicated that the optimal incubation time was 45 min (Fig. S5). To investigate the mechanism of the materials for separation and identification of phosphorylated peptides, β-CD-COF was used to enrich phosphopeptides under the same conditions. Before enrichment (Fig. S6a), non-phosphorylated peptide peaks dominated the spectrum.

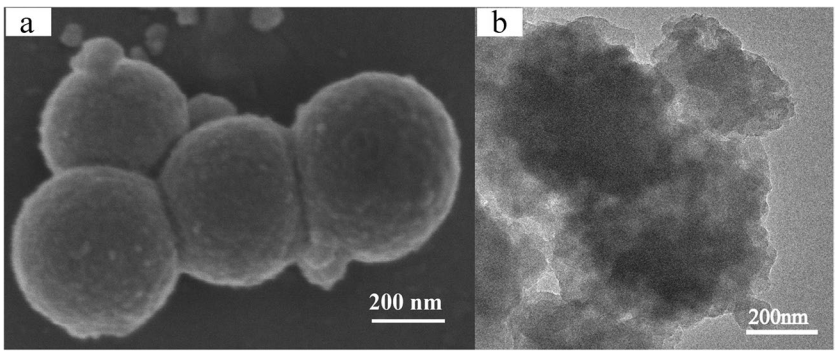

Fig. 2 **a** SEM image of β-CD-COF@Ti^{4+}; **b** TEM image of β-CD-COF@Ti^{4+}

After enrichment by β-CD-COF, only 1 phosphopeptide could be observed (Fig. S6b). Besides, the background baseline of the mass spectrum was relatively high. Then, after enrichment by β-CD-COF@Ti^{4+}, 13 phosphopeptides could be observed (Fig. S6c), and the detailed information about phosphorylated peptides was listed in Table S1. The result indicated that the mechanism of the materials for separation and identification of phosphorylated peptides was mainly based on the coordination of Ti^{4+} and phosphate groups.

The β-casein digests were diluted to different concentrations (500, 50, 5, and 0.5 fmol) to explore the detection limit of β-CD-COF@Ti^{4+} towards phosphopeptides. After diluting the β-casein concentration to 500 fmol, 6 phosphopeptides with S/N > 3 were captured by β-CD-COF@Ti^{4+} (Fig. S7a). Five phosphopeptide peaks with S/N > 3 could be observed when diluting the β-casein digests to 50 fmol (Fig. S7b). Two phosphopeptide peaks (Fig. S7c) with S/N > 3 were also seen at a concentration of 5 fmol. Additionally, even the concentration down to 0.5 fmol, 1 phosphopeptide peak (m/z = 2062.8, S/N > 3) could be observed (Fig. S7d). Based on the above analysis, β-CD-COF@Ti^{4+} showed low detection for phosphopeptides.

BSA digests were used as the interfering peptides to verify the selectivity of β-CD-COF@Ti^{4+} towards phosphopeptides. When the BSA/β-casein at molar ratio was 100:1, 7 phosphopeptide peaks dominated the spectrum (Fig. S8a). When the molar ratio was 250:1, 5 phosphopeptide peaks were observed (Fig. S8b). Three phosphopeptide peaks (Fig. S8c) were observed with the molar ratio that was 500:1. A single phosphopeptide peak was still identified at a molar ratio of 1000:1 (Fig. S8d). These results demonstrated the good selectivity of β-CD-COF@Ti^{4+}.

The peak intensity changes of three typical phosphopeptides (m/z = 2062, 2556, 3123) were used to assess the phosphopeptide loading capacity of β-CD-COF@Ti^{4+}. Each experiment was performed 3 times, and the RSDs were given in Table S2. The experiment was performed by changing the amount of β-CD-COF@Ti^{4+} and fixing the quantity of β-casein digests (10 μg). With an increasing amount of β-CD-COF@Ti^{4+}, the intensity of the peaks also increased (Fig. S9). The peak intensity was almost stable when the mass of β-CD-COF@Ti^{4+} was 100 μg, and the peak intensity was almost stable when the amount of material further increased. The loading capacity of β-CD-COF@Ti^{4+} was approximately 100 $mg \cdot g^{-1}$ by calculating the formula $Q = m_1/m_2$ (m_1 represents the amount of β-casein digests, and m_2 represents the amount of material).

A comparison of the relevant properties of our work with recently reported IMAC nanomaterials is given in Table S3. Benefiting from the selection of organic ligands, β-CD-COF@Ti^{4+} exhibited superior performance on the enrichment of phosphopeptides, such as a low detection limit, high sensitivity, and high loading capacity. Am7CD could be grafted with more organic ligands (THBA, TPA) due to its abundant amino groups; the structural unit THBA introduced in the β-CD-COF framework had multiple hydroxyl affinity sites, which provided a platform for the subsequent binding of more metal ions (Ti^{4+}) and improved the hydrophilicity of material. In addition, compared with Fe_3O_4@mPDA@Ti^{4+}, β-CD-COF@Ti^{4+} had a higher loading capacity due to its large specific area. Excitingly, there were few reports on the application of Ti^{4+} functionalized β-cyclodextrin covalent organic frameworks in proteomics. Therefore, the effective building of β-CD-COF@Ti^{4+} provided a feasible route for the construction of functionalized β-cyclodextrin COF and a platform for the enrichment of phosphopeptides.

Application of β-CD-COF@Ti^{4+} for the enrichment of phosphopeptides from complex bio-samples

Defatted milk is a classic biological sample containing phosphoproteins. Based on the above results, β-CD-COF@Ti^{4+} was further used to detect phosphopeptides in defatted milk. Before treatment with β-CD-COF@Ti^{4+}, no phosphopeptides were observed, and non-phosphopeptides dominated the spectrum (Fig. S10a). After treatment with β-CD-COF@Ti^{4+}, nine phosphopeptides of high mass intensity and a clear background were observed (Fig. S10b). Detailed information was presented in Table S4. In summary, the results of the study on complex samples provided strong proof for the good performance of the obtained materials on the capture of phosphopeptides.

Serum is a typical clinical specimen that contains a large number of substances necessary for life activities, such as endogenous peptides and proteins. From the current research status and disease characteristics, the discovery of specific proteins related to disease lesions could be used to assist in the diagnosis of diseases, and it was important for the elaboration of relevant diseases. After treatment with β-CD-COF@Ti^{4+}, 29 phosphopeptides related to 23 phosphoproteins from the normal control group and 24 phosphopeptides related to 22 phosphoproteins in the uremia patient group were detected (Fig. S11), respectively. As shown in Fig. 3a, a total of 23 phosphorylation sites, 21 phosphopeptides, and 18 phosphoproteins were only detected in normal samples. By comparison, a total of 20 phosphorylation sites, 17 phosphopeptides, and 16 phosphoproteins were detected only in uremia samples. The relevant information was in supporting information Table S5 and S6.

To assess the significant differences between healthy controls and uremia patients, we centered on the phosphorylation sites and visualized the amino acid frequencies through WebLogo. By comparing the results of normal and uremic patients (Fig. 3b), we found no significant differences in the phosphorylation sites among the three main amino acids (tyrosine, threonine, and serine). Notably, the possibility

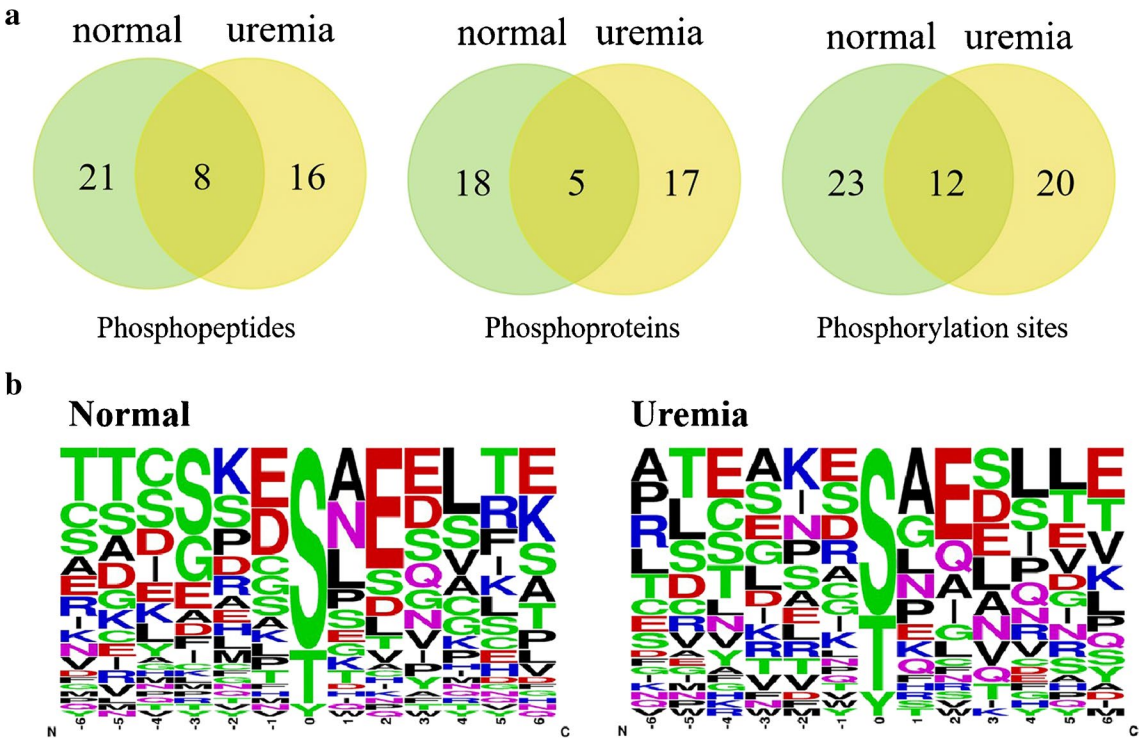

Fig. 3 **a** Venn diagram of phosphopeptides, phosphoproteins, and phosphorylation sites of normal control and uremia patient; **b** the sequence logo of identified phosphopeptides from normal control and uremia patient

of valine, leucine, and isoleucine near the phosphorylation sites was greatly increased in patients with uremia, and the changes in these metabolites may be related to the pathogenesis of uremia, which may have actual significance for the clinical diagnosis and treatment of uremia [25].

Besides, the terms of Gene Ontology (GO) analysis were conducted to distinguish the phosphoproteins of the two samples through the DAVID database v6.8, in an attempt to explore valuable biological information from the perspectives of molecular function, cellular component, and biological process (Fig. 4). From the molecular function, uremia patients were often accompanied by altered lipoprotein metabolic processes. Abnormal lipoprotein metabolism was common in uremia and significantly affected the development of kidney-related diseases. [26, 27]. As can be seen from the cellular component, very-low-density lipoprotein (VLDL) particle and high-density lipoprotein (HDL) particle are highly expressed in the serum of uremia patients. According to previous reports, the VLDL particles in dialysis patients contain more cholesterol and phospholipids than healthy controls [28]. In addition, the high-density lipoprotein (HDL) particles of uremic patients have changed, which may lead to their loss of vascular protection function and conversion into inflammatory particles, leading to further development of the disease [29, 30]. From the biological process perspective, lipid binding is thought to be closely associated with phosphoproteins in the serum of uremic patients. It has been reported that renal dysfunction in uremia patients may affect lipid binding activity, thereby affecting the entire lipid metabolism process [31]. In summary, the pathological process of uremia may involve these functional pathways, which is instructive for relevant diagnosis and treatment.

Application of β-CD-COF@Ti^{4+} for the enrichment of exosomes from serum

We further applied β-CD-COF@Ti^{4+} in the enrichment of exosomes. As shown in the TEM image (Fig. 5a), the morphology of exosomes captured by β-CD-COF@Ti^{4+} was spherical in structure with a diameter of about 30–150 nm, in good agreement with the previous articles [32–34]. To investigate the mechanism of the materials for separation and identification of exosomes, β-CD-COF was used to enrich exosomes under the same conditions. Besides, western blot further validated the promising application of two materials (β-CD-COF and β-CD-COF@Ti^{4+}) in the isolation and enrichment of exosomes. After enrichment by β-CD-COF, three marker proteins (CD9, CD63, TSG101) of exosomes were barely observed (Fig. 5b). By contrast, after enrichment by β-CD-COF@Ti^{4+}, three marker proteins (CD9, CD63,

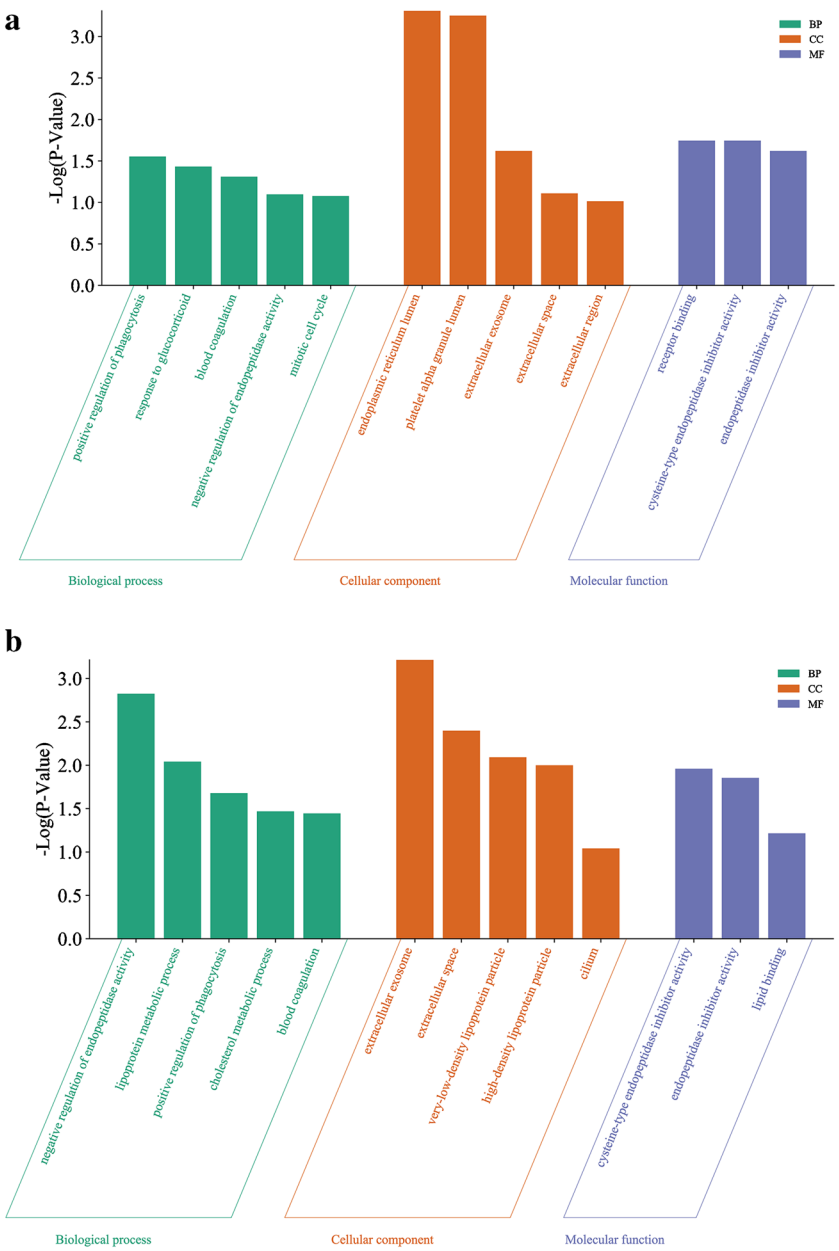

Fig. 4 The GO analysis of phosphoproteins identified in the serum of normal control (**a**) and uremia patient (**b**)

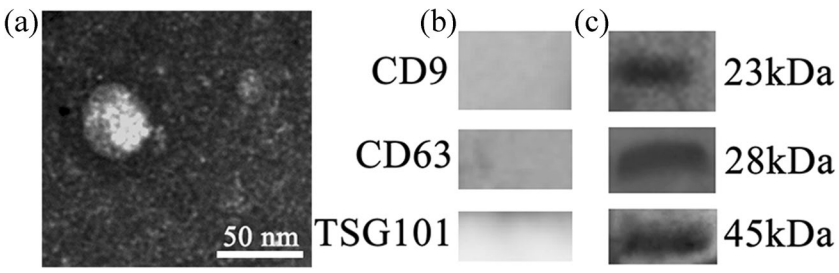

Fig. 5 **a** TEM image of exosomes captured by β-CD-COF@Ti^{4+}; western blot results of marker proteins in exosomes after enrichment by **b** β-CD-COF and **c** β-CD-COF@Ti^{4+}

TSG101) of exosomes were detected (Fig. 5c) [35]. β-CD-COF@Ti^{4+} could capture exosomes through the adsorption of metal ions towards the phospholipid layer, based on the IMAC strategy. In other words, β-CD-COF@Ti^{4+} has great potential for applications in the capture and separation of exosomes.

Conclusions

All in all, we developed a β-cyclodextrin covalent organic framework by a new synthetic process. The presence of sufficient cis dihydroxyl groups on the β-CD-COF layer allowed for more chelation of Ti^{4+}, providing a better platform based on the IMAC strategy for the separation of phosphorylated peptides and exosomes from biological samples. β-CD-COF@Ti^{4+} showed excellent selectivity, low detection limit, and good ability towards phosphopeptides. The limitation of this strategy is the use of organic reagents, so exploration of an environmental-friendly synthesis method is needed in the future phosphoproteomics research.

Supplementary Information The online version contains supplementary material available at https://doi.org/10.1007/s00604-023-05952-3.

Acknowledgements This work is supported by the Natural Science Foundation of Zhejiang Province (LY22B050008).

Data availability All relevant data is within the figures and supporting information.

Declarations

Conflict of interest The authors declare no competing interests.

References

1. Zhu J, Liu ZX, Wang L, Jin QS, Zhao YP, Du AT, Ding N, Wang Y, Jiang H, Zhu L (2022) Exosome mimetics-loaded hydrogel accelerates wound repair by transferring functional mitochondrial proteins. Front Bioeng Biotech 10:866505. https://doi.org/10.3389/fbioe.2022.866505
2. Wang BC, Xie ZH, Ding CF, Deng CH, Yan YH (2023) Recent advances in metal oxide affinity chromatography materials for phosphoproteomics. TrAC-Trends Anal Chem 158:116881. https://doi.org/10.1016/j.trac.2022.116881
3. Zhang N, Sun NR, Deng CH (2021) Rapid isolation and proteome analysis of urinary exosome based on double interactions of Fe_3O_4@TiO_2-DNA aptamer. Talanta 221:121571. https://doi.org/10.1016/j.talanta.2020.121571
4. Saraswat M, Joenvaara S, Musante L, Peltoniemi H, Holthofer H, Renkonen R (2015) N-linked (N-) glycoproteomics of urinary exosomes. Mol Cell Proteomics 14:263–276. https://doi.org/10.1074/mcp.M114.040345
5. Melo SA, Luecke LB, Kahlert C, Fernandez AF, Gammon ST, Kaye J, LeBleu VS, Mittendorf EA, Weitz J, Rahbari N, Reissfelder C, Pilarsky C, Fraga MF, Worms DP, Kalluri R (2015) Glypican-1 identifies cancer exosomes and detects early pancreatic cancer. Nature 523:177–U82. https://doi.org/10.1038/nature14581
6. Donoso-Quezada J, Ayala-Mar S, Gonzaez-Valdez J (2021) The role of lipids in exosome biology and intercellular communication: function, analytics and applications. Traffic 22:204–220. https://doi.org/10.1111/tra.12803
7. Kimiz-Gebologlu I, Oncel SS (2022) Exosomes: large-scale production, isolation, drug loading efficiency, and biodistribution and uptake. J Control Release 347:533–543. https://doi.org/10.1016/j.jconrel.2022.05.027
8. Iraci N, Leonardi T, Gessler F, Vega B, Pluchino S (2016) Focus on extracellular vesicles: physiological role and signalling properties of extracellular membrane vesicles. Int J Mol Sci 17:171. https://doi.org/10.3390/ijms17020171
9. Wang BC, Liu B, Yan YH, Tang KQ, Ding CF (2019) Binary magnetic metal-organic frameworks composites: a promising affinity probe for highly selective and rapid enrichment of mono- and multi-phosphopeptides. Microchim Acta 186:832. https://doi.org/10.1007/s00604-019-3916-5
10. Xu ZX, Wu YL, Hu XF, Deng CH, Sun NR (2022) Inherently hydrophilic mesoporous channel coupled with metal oxide for fishing endogenous salivary glycopeptides and phosphopeptides. Chin Chem Lett 33:4695–4699. https://doi.org/10.1016/j.cclet.2021.12.069
11. Zhang N, Sun NR, Deng CH (2020) A hydrophilic magnetic MOF for the consecutive enrichment of exosomes and exosomal phosphopeptides. Chem Commun 56:13999–14002. https://doi.org/10.1039/d0cc06147f
12. Ogami K, Suzuki HI (2021) Nuclear RNA exosome and pervasive transcription: dual sculptors of genome function. Int J Mol Sci 22:13401. https://doi.org/10.3390/ijms222413401
13. Zhang N, Hu XF, Chen HL, Deng CH, Sun NR (2021) Specific enrichment and glycosylation discrepancy profiling of cellular exosomes using a dual-affinity probe. Chem Commun 57:6249–6252. https://doi.org/10.1039/d1cc01530c
14. Sun NR, Yu HL, Wu H, Shen XZ, Deng CH (2021) Advanced nanomaterials as sample technique for bio-analysis. TrAC-Trends Anal Chem 135:116168. https://doi.org/10.1016/j.trac.2020.116168
15. Du JL, Tian HH, Fu MY, Yan YH, Wang C, Ding CF (2022) Post-modified porous hollow nanospheres incorporating multiple strategies for comprehensive phosphoproteomics analysis of serum of Alzheimer's disease. Microporous Mesoporous Mater 341:112066. https://doi.org/10.1016/j.micromeso.2022.112066
16. Hu XF, Li YL, Miao AZ, Deng CH (2020) Dual metal cations coated magnetic mesoporous silica probe for highly selective capture of endogenous phosphopeptides in biological samples. Microchim Acta 187:7. https://doi.org/10.1007/s00604-020-04323-6
17. Jia SC, Tang RZ, Zhang S, Gao Z, Gong BL, Ma SJ, Ou JJ (2022) Design and fabrication of reusable core-shell composite microspheres based on nanodiamond for selective enrichment of phosphopeptides. Microchim Acta 189:124. https://doi.org/10.1007/s00604-022-05234-4
18. Fang XW, Liu XG, Sun NAR, Deng CH (2021) Enhanced specificity of bimetallic ions via mesoporous confinement for phosphopeptides in human saliva. Talanta 233:122587. https://doi.org/10.1016/j.talanta.2021.122587
19. Wang B, Wang BC, Feng QS, Fang X, Dai XH, Yan YH, Ding CF (2022) Magnetic guanidyl–functionalized covalent organic framework composite: a platform for specific capture and isolation of phosphopeptides and exosomes. Microchim Acta 189:1–9. https://doi.org/10.1007/s00604-022-05394-3
20. Wu YL, Sun NR, Deng CH (2020) Construction of magnetic covalent organic frameworks with inherent hydrophilicity for efficiently enriching endogenous glycopeptides in human saliva. ACS Appl Mater Interfaces 12:9814–9823. https://doi.org/10.1021/acsami.9b22601
21. Wang XH, Wu JQ, Liu X, Qiu X, Cao LQ, Ji YB (2022) Enhanced chiral recognition abilities of cyclodextrin covalent organic frameworks via chiral/achiral functional modification. ACS Appl Mater Interfaces 14:25928–25936. https://doi.org/10.1021/acsami.2c05572
22. Lu SY, Wang SL, Wu PA, Wang DQ, Yi JC, Li L, Ding P, Pan HZ (2021) A composite prepared from covalent organic framework and gold nanoparticles for the electrochemical determination of

enrofloxacin. Adv Powder Technol 32:2106–2115. https://doi.org/10.1016/j.apt.2021.04.025
23. Wang XH, Yu JL, Yang HD, Shen J, Liu HL, Zhou JH (2021) A new Ti-based IMAC nanohybrid with high hydrophilicity and enhanced absorption capacity for the selective enrichment of phosphopeptides. J Chromatogr B 1179:122851. https://doi.org/10.1016/j.jchromb.2021.122851
24. Wei HX, Chen JY, Wang SL, Fu FH, Zhu X, Wu CY, Liu ZJ, Zhong GX, Lin JH (2019) A nanodrug consisting of doxorubicin and exosome derived from mesenchymal stem cells for osteosarcoma treatment in vitro. Int J Nanomedicine 14:8603–8610. https://doi.org/10.2147/IJN.S218988
25. Wang ZZ, Wei BB, Chen Z, Zhu HW, Shen GP, Feng JH (2018) H-1 nuclear magnetic resonance-based investigation of uremia by metabolomic analysis. Chin J Anal Chem 46:1415–1423. https://doi.org/10.11895/j.issn.0253.3820.181286
26. Telci A, Salmayenli N, Aydin AE, Yamaner S, Sivas A, Eldegez U (1992) Serum lipids and apolipoprotein concentrations and plasma fibronectin concentrations in renal transplant patients. Eur J Clin Chem Clin Biochem 30:847–850. https://doi.org/10.1515/cclm.1992.30.12.847
27. Bergesio F, Monzani G, Ciuti R, Pinzani P, Fiaschi N, Priami F, Cirami C, Ciccarelli C, Salvadori M (1998) Total antioxidant capacity (TAC): is it an effective method to evaluate the oxidative stress in uraemia? J Biolumin Chemilumin 13:315–319. https://doi.org/10.1002/(SICI)1099-1271(1998090)13:5<315::AID-BIO491>3.0.CO;2-6
28. Amadottir M, Dallongeville J, Fruchart JC, NilssonEhle P (1996) Very-low-density lipoprotein of uremic patients is a poor substrate for bovine lipoprotein lipase in vitro. Metab Clin Exp 45:686–690. https://doi.org/10.1016/S0026-0495(96)90132-8
29. Kaesler N, Schreibing F, Speer T, de la Puente-Secades S, Rapp N, Drechsler C, Kabgani N, Kuppe C, Boor P, Jankowski V, Schurgers L, Kramann R, Floege J (2022) Altered vitamin K biodistribution and metabolism in experimental and human chronic kidney disease. Kidney Int 101:338–348. https://doi.org/10.1016/j.kint.2021.10.029
30. Mirjam S, Markus T, van der Markus G (2015) High-density lipoprotein: structural and functional changes under uremic conditions and the therapeutic consequences. Handb Exp Pharmacol 224:424–453. https://doi.org/10.1007/978-3-319-09665-0_13
31. Moestrup SK, Nielsen LB (2005) The role of the kidney in lipid metabolism. Curr Opin Lipidol 16:301–306. https://doi.org/10.1097/01.mol.0000169350.45944.d4
32. Wu YL, Zhang N, Wu H, Sun NR, Deng CH (2021) Magnetic porous carbon-dependent platform for the determination of N-glycans from urine exosomes. Microchim Acta 188:6. https://doi.org/10.1007/s00604-021-04728-x
33. Liu ZQ, Zhang XG, Yu QG, He JJ (2014) Exosome-associated hepatitis C virus in cell cultures and patient plasma. Biochem Biophys Res Commun 455:218–222. https://doi.org/10.1016/j.bbrc.2014.10.146
34. Kim JY, Rhim WK, Yoo YI, Kim D, Ko KW, Heo Y, Park CG, Han DK (2021) Defined MSC exosome with high yield and purity to improve regenerative activity. J Tissue Eng 14:263–276. https://doi.org/10.1074/mcp.M114.040345
35. Lv YN, Chen J, Hu JF, Qian YS, Kong Y, Fu LS (2021) Non-muscle myosin heavy chain IIA-mediated exosome release via regulation of the rho-associated kinase 1/myosin light chains/actin pathway. Front Pharmacol 11:598592. https://doi.org/10.3389/fphar.2020.598592